physica status solidi

pss

www.pss-journals.com

reprint

WILEY-VCH

Phys. Status Solidi C **11**, No. 3–4, 644–647 (2014) / **DOI** 10.1002/pssc.201300413

physica status solidi c
www.pss-c.com
current topics in solid state physics

Fabrication of nitride/Si tandem cell structures with low environmental burden by surface activated bonding

Naoteru Shigekawa[*,1], Jianbo Liang[1], Noriyuki Watanabe[2], and Akio Yamamoto[3]

[1] Graduate School of Engineering, Osaka City University, 3-3-138, Sugimoto, Sumiyoshi, Osaka 558-8585, Japan
[2] NTT Photonics Labs., Nippon Telegraph and Telephone Corporation, 3-1, Morinosato-Wakamiya, Atsugi, Kanagawa 243-0198, Japan
[3] University of Fukui, 3-9-1, Bunkyo, Fukui 910-8507, Japan

Received 15 August 2013, revised 14 October 2013, accepted 7 January 2014
Published online 6 March 2014

Keywords surface activated bonding, tandem solar cell, GaN substrate, open-circuit voltage, Si substrate

* Corresponding author: e-mail shigekawa@elec.eng.osaka-cu.ac.jp, Phone: +81-6-6605-2676, Fax: +81-6-6605-2676

Group-III nitride on Si tandem solar cell structures, which are free from materials with high impacts on the environment such as group-III arsenides or phosphides, were successfully fabricated using the surface-activated bonding of nitride-based sub cells, which had been grown on (0001) GaN substrates, and (111) Si-based sub cells. The backsides of the GaN substrates had been polished and their averaged roughness was smaller than 1 nm prior to bonding. The open-circuit voltage (V_{OC}) of the tandem cells was almost equal to the sum of V_{OC} of the respective sub cells, while the conversion efficiency was limited by the properties of the nitride-based top cells. Nitride-on-(100) Si tandem cells were also fabricated and the enhancement in V_{OC} was observed.

© 2014 WILEY-VCH Verlag GmbH & Co. KGaA, Weinheim

1 Introduction Compound-semiconductor-based tandem (multi junction) solar cells, which are composed of stacks of sub cells with different bandgaps, are promising as practical candidates for next-generation solar cells [1–3] since tandem cells have reportedly produced higher conversion efficiencies in comparison with other solar cell structures [4]. The strategy for realising high efficiencies in the tandem cells is to slice the solar spectrum into several parts and absorb the respective parts by using sub cells. The bandgap of each sub cell is determined so that the current matching condition is fulfilled. In most cases the sub cells are made of group-III arsenides or phosphides with specified bandgaps. InGaP/(In)GaAs/Ge triple junction cells have reportedly produced conversion efficiencies $> 30\%$ [1–3].

Noting that the group-III arsenides and phosphides potentially bring about a large impact on the environment, they should be preferably replaced by materials with lower environmental burdens. Possible candidates for them are group-III nitrides with bandgaps varied between 0.7 (InN) and 6.2 (AlN) eV [5]. The possibility of nitrides as constituent of solar cells has widely been explored [5–11]. Furthermore Si-based cells should be substituted for Ge-based bottom cells in the triple junction cells for lowering the costs of cells. A pioneering work for the growth of GaN-based cells on Si-based cells using the plasma-assisted molecular-beam epitaxy was reported [7]. Researches on the growth of InGaN-based cells on Si-based cells are in progress [11].

Given that the growth of nitride-based solar cell structures on Si substrates is still hard technological issues, other approaches, the mechanical-stacking (hybrid tandem) approaches [12–14], should be explored for realising the nitride-on-Si stacks. The surface-activated bonding (SAB), in which the native oxide layers formed on surfaces of substrates are removed by Ar beam irradiation prior to bonding [15, 16], is one of the promising methods for the hybrid tandem approaches. The present authors previously applied SAB for making junctions of a variety

© 2014 WILEY-VCH Verlag GmbH & Co. KGaA, Weinheim

of dissimilar materials and examined their structural and electrical characteristics [17–19].

In this work, we fabricated hybrid tandem cells composed of InGaN/GaN multi quantum wells (MQWs) based top cells and Si-based bottom cells by using SAB and examined the applicability of SAB for realising nitride-on-Si tandem cells.

2 Results and dicussions

2.1 Sample preparation On n-type (0001) GaN substrates with a carrier concentration of $\sim 10^{18}$ cm^{-3}, we grew 100 nm-thick n-doped GaN buffer layers ($\sim 5 \times 10^{18}$ cm^{-3}), undoped 10 pairs of InGaN/GaN MQWs, and p-doped emitter/contact layers in this sequence. By using Xray-diffraction analyses, the thicknesses of InGaN well layers and GaN barrier layers in MQWs were found to be 3.4 and 5.8 nm, respectively. Furthermore the InN mole fraction of InGaN well layers was estimated to be 0.14. We made the emitter contacts on the contact layers by Ni/Au evaporation. Next the base contacts were formed on the surfaces of the n-GaN buffer layers, which had been exposed by mesa etching, by evaporating Ti/Al/Ni/Au and an annealing at 800 °C for 60 s so that the nitride-based top cells were fabricated. The area of the mesa was $1\ \mathrm{mm}^2$. Details of growth and characterisation of the layer structure as well as the cell fabrication process were previously reported [10]. By polishing the backsides of substrates, their averaged roughness was improved from 170 nm (before polishing) to 0.33 nm (after polishing) as is shown in Fig. 1(a). We then diced the GaN substrates into $1\ \mathrm{cm}^2$ chips.

Si-based bottom cell structures were made by the implantation of boron (B) ions to high-resistive n-type (111) and (100) Si substrates and subsequent rapid thermal annealing at 900 °C for 60 s. The acceleration energy in the ion implantation was 10 keV. The preparatory SIMS measurements suggested that the profile of the concentration of B atoms revealed a peak with a height of $\approx\ 1.5 \times 10^{20}$ cm^{-3} at a depth of $\approx\ 50\ \mathrm{nm}$ after the annealing. We also formed n^+ layers on the backsides of Si substrates by means of the ion-implantation of phosphors (P) and annealing for obtaining good ohmic contacts and back-surface-field layers. The base contacts to Si-based bottom cells were achieved by Ti/Au evaporation. Furthermore, standalone Si-based cells were fabricated by forming the emitter contacts by evaporating Al and annealing at 400 °C for 60 s.

After the surface activation process using the Ar beam, the backsides of GaN substrates were bonded to the top surfaces of Si-based bottom cells in the atmospheric pressure of $\sim 10^{-6}$ Pa. The samples were not intentionally heated during the bonding process. The bonding pressure was ~ 10 MPa. Both of the nitride-on-(111)-Si and (100)-Si tandem cells were successfully fabricated thank to the improved smoothness of backside of GaN substrates. The schematic cross section of the tandem cells is shown in Fig. 1(b). It is noteworthy that the characteristics of the tandem cells as well as those of the top cells, which are parts of the tandem cells, are independently measured since the base contacts to the top cells were formed.

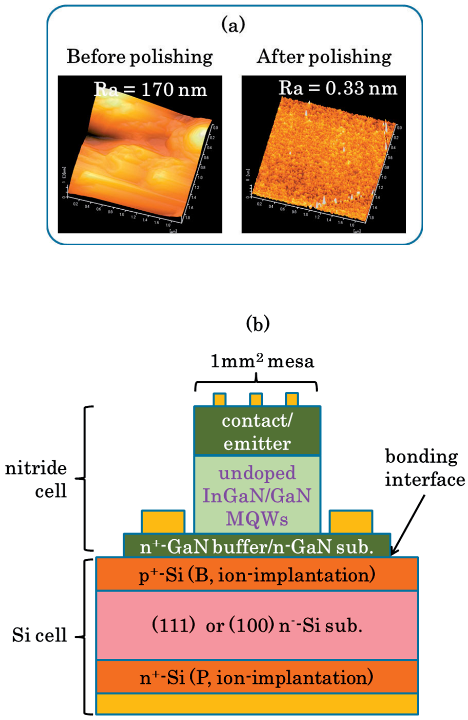

Figure 1 (a) AFM images of backsides of GaN substrates before and after polishing. (b) A schematic cross section of nitride-on-Si tandem cells fabricated by using SAB.

2.2 Cell characterisation We measured current-voltage ($I-V$) characteristics of cells under air mass 1.5G and one sun conditions using an in-house solar simulator. The measurements were performed at room temperature. The characteristics of three neighbouring nitride-on-(111)-Si tandem cells as well as the constituent top cells are shown in Figs. 2(a) to 2(c). The characteristics of the separately fabricated (111)-Si based bottom cells are shown in Fig. 2(d). Results for nitride-on-(100)-Si cells and (100)-Si based bottom cells are shown in Figs. 3(a) and 3(b), respectively .

The $I-V$ characteristics shown in Fig. 2(a) reveal that the short circuit current (J_{SC}), the open circuit voltage (V_{OC}), the series and shunt resistances (R_{ser} and R_{sh}), and the efficiency are $0.22\ \mathrm{mA/cm}^2$, 1.64 V, $3.2{\times}10^3\ \Omega\mathrm{cm}^2$, $4.0{\times}10^4\ \Omega\mathrm{cm}^2$, and 0.16%, respectively. Those for the nitride top cells are $0.21\ \mathrm{mA/cm}^2$, 1.12 V, $3.1{\times}10^3\ \Omega\mathrm{cm}^2$, $2.1{\times}10^4\ \Omega\mathrm{cm}^2$, and 0.08%, respectively. Similar values are obtained from $I-V$ characteristics shown in Figs. 2(b) and 2(c). From the characteristics of the (111)-Si based bottom cell [Fig. 2(d)] we extract J_{SC} of $24.0\ \mathrm{mA/cm}^2$, V_{OC} of 0.56 V, R_{ser} of $0.55\ \Omega\mathrm{cm}^2$,

© 2014 WILEY-VCH Verlag GmbH & Co. KGaA, Weinheim

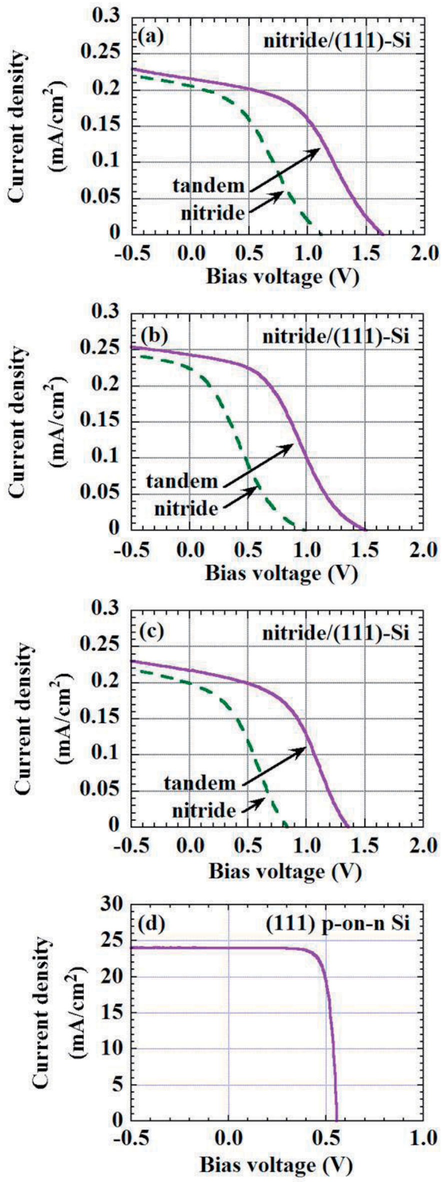

Figure 2 (a)-(c) $I-V$ characteristics of neighbouring nitride-on-(111)-Si tandem cells as well as those of constituent top cells. (d) $I-V$ characteristics of a separately-fabricated (111)-Si based cell.

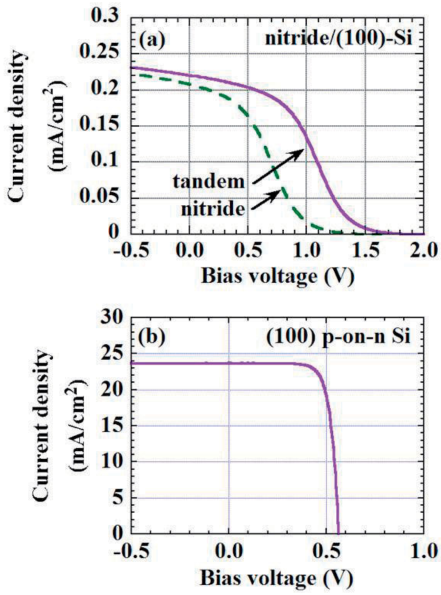

Figure 3 $I-V$ characteristics of (a) a nitride-on-(100)-Si tandem cell and (b) a separately-fabricated (100)-Si based cell.

R_{sh} of $7.4{\times}10^4\ \Omega\mathrm{cm}^2$, and the efficiency of 10.4%. The magnitude of R_{ser} of the tandem cells is much larger than the resistance across the bonding interfaces, which was estimated to be $\sim 10^2\ \Omega\mathrm{cm}^2$ as is discussed later. The measured series resistance of the tandem cells is, consequently, likely to be attributable to the resistance on the p-GaN emitter contacts of the top cells.

We find that in the nitride-on-(111)-Si tandem cells the sum of V_{OC} of the top cell and that of the bottom cell is in almost agreement with V_{OC} of the tandem cell. This means that the two sub cells are electrically well-connected to each other through the bonding interfaces. V_{OC} of the nitride-on-(100)-Si tandem cell, 1.88 V as is seen from Fig. 3(a), is slightly lower than the sum of V_{OC} of the top cell (1.50 V) and that of the bottom cell (0.56 V from Fig. 3(b)). The origin of the discrepancy remains unclear.

We have to note that J_{SC} of the nitride-based cells, which is much lower than J_{SC} of the (111)- and (100)-Si based cells, limits the performances of the tandem cells, which suggests that the quality of the top cell must be improved. In addition, the occurrence of the difference in J_{SC} between the nitride and Si-based cells implies that when the tandem cells are short circuited the bottom cells are forward biased by ~ 0.5 V, which should amount to the change in the self bias voltage applied to R_{sh} of the top cells ($2.1 \times 10^4\ \Omega\mathrm{cm}^2$) and R_{ser} ($3.2 \times 10^3\ \Omega\mathrm{cm}^2$) from the case for the standalone top cells. The increase in J_{SC} of the tandem cells in comparison with that of the top cells is qualitatively explained in such scheme.

2.3 Conduction across bonding interfaces The $I-V$ characteristics measured between the base contacts of top and bottom cells on (111) Si and (100) Si substrates without illumination are shown in Fig. 4. The $I-V$ characteristics, which are assumed to reflect the electrical conduction across the bonding interfaces, reveal quasi-ohmic properties with a resistance of $\sim 200\ \Omega\mathrm{cm}^2$ for the tandem cells on (111) Si substrates. The slope of the characteristics for the tandem cells on (100) Si substrates corresponds to a resistance of $\sim 140\ \Omega\mathrm{cm}^2$ although the characteristics are slightly unsymmetrical.

© 2014 WILEY-VCH Verlag GmbH & Co. KGaA, Weinheim

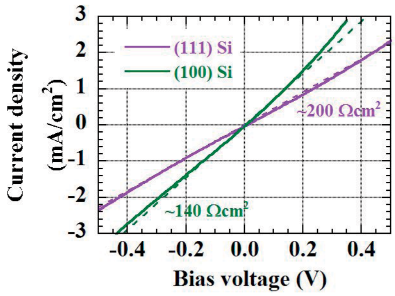

Figure 4 $I - V$ characteristics between base contacts of top and bottom cells in nitride-on-(111) Si and nitride-on-(100) Si tandem cells measured without illumination.

In contrast, given that the conduction-band discontinuity at the GaN/Si interface is assumed to be zero ($\Delta E_C \approx 0$ eV) [5], the thickness of the depletion layer in n-GaN of the n-GaN/p-Si junctions should be $\sim$ 30 nm. This suggests that the conductive properties across the bonding interfaces should be unsymmetrical and their resistance is large so that the operation of the tandem cells might be degraded. The conductive characteristics of the actual n-GaN/p-Si junctions might be attributable to interface states possibly introduced through the bonding process. Note that similar properties were observed in GaN/GaAs junctions obtained using the wafer fusion [20]. The resistance across the interface might be lowered by increasing the concentration of impurities in GaN substrates [19].

Although the mechanism inducing such quasi-ohmic properties in the GaN/Si junctions remains unclear, the achieved results implies that SAB provides a good interface between the nitride and Si-based sub cells. Structures and fabrication processes of the respective sub cells can be separately optimised for obtaining better performances of the tandem cells. Also by noting that nitride top cells are successfully bonded to the bottom cells based on (100)-Si substrates, which are widely used than (111)-Si substrates in the present semiconductor industries, SAB is assumed to play a major role in accelerating the research and development for nitride-on-Si tandem solar cells with high efficiencies, low costs, and low environmental burdens.

3 Conclusions Using the surface activated bonding, we fabricated nitride-on-Si hybrid tandem cell structures of nitride top cells on GaN substrates and (111)- and (100)-Si bottom cells. The GaN substrates was successfully bonded to the surfaces of Si bottom cells thank to the improved smoothness of the polished backside of GaN substrates. The open-circuit voltage (V_{OC}) of tandem cells on (111) Si was almost in agreement with the sum of V_{OC} of the respective sub cells.

Acknowledgements The authors are grateful to M. Morimoto and S. Nishida for their assistance in sample preparation and characterisation. This work was supported by “Creative Research for Clean Energy Generation Using Solar Energy”project in Core Research for Evolutional Science and Technology (CREST) program of Japan Science and Technology Agency (JST).

References

[1] T. Takamoto, E. Ikeda, and H. Kurita, Appl. Phys. Lett. **70**, 381 (1997).
[2] T. Takamoto, M. Kaneiwa, M. Imaizumi, and M. Yamaguchi, Prog. Photovolt.: Res. Appl. **13**, 495 (2005).
[3] J. F. Geisz, S. Kurtz, M. W. Wanlass, J. S. Ward, A. Duda, D. J. Friedman, J. M. Olson, W. E. McMahon, T. E. Moriarty, and J. T. Kiehl, Appl. Phys. Lett. **91**, 023502 (2007).
[4] L. L. Kazmerski, ftp://ftp2.nrel.gov/pub/ewc-keei/Paper2_and_PPT2_Kazmerski_(final).pdf.
[5] J. W. Ager III, L. A. Reichertz, K. M. Yu, W. J. Schaff, T. L. Williamson, M. A. Hoffbauer, N. M. Haegel, and W. Walukiewicz, Proc. 33rd IEEE Photovoltaic Specialists Conference, San Diego, USA (IEEE, 2008), DOI 10.1109/PVSC.2008.4922663.
[6] A. Yamamoto, K. Sugita, M. Horie, Y. Ohmura, M R. Islam, and A. Hashimoto, Proc. 33rd IEEE Photovoltaic Specialists Conference, San Diego, USA (IEEE, 2008), DOI 10.1109/PVSC.2008.4922870.
[7] L. A. Reichertz, I. Gherasoiu, K. M. Yu, V. M. Kao, W. Walukiewicz, and J. W. Ager III, Appl. Phys. Express **2**, 122202 (2009).
[8] Y. Kuwahara, T. Fujii, T. Sugiyama, D. Iida, Y. Isobe, Y. Fujiyama, Y. Morita, M. Iwaya, T. Takeuchi, S. Kamiyama, I. Akasaki, and H. Amano, Appl. Phys. Express **4**, 021001 (2011).
[9] L. Sang, M. Liao, N. Ikeda, Y. Koide, and M. Sumiya, Appl. Phys. Lett. **99**, 161109 (2011).
[10] N. Watanabe, H. Yokoyama, N. Shigekawa, K. Sugita, and A. Yamamoto, Jpn. J. Appl. Phys. **51**, 10ND10 (2012).
[11] A. G. Bhuiyan, A. Mihara, T. Esaki, K. Sugita, A. Hashimoto, A. Yamamoto, N. Watanabe, H. Yokoyama, and N. Shigekawa, Phys. Status Solidi C **9**, 670 (2012).
[12] M. J. Archer, D. C. Law, S. Mesropian, M. Haddad, C. M. Fetzer, A. C. Ackerman, C. Ladous, R. R. King, and H. A. Atwater, Appl. Phys. Lett. **92**, 103503 (2008).
[13] H. Mizuno, K. Makita, and K. Matsubara, Appl. Phys. Lett. **101**, 191111 (2012).
[14] K. Tanabe, K. Watanabe, and Y. Arakawa, Sci. Rep. **2**, 349 (2012).
[15] H. Takagi, K. Kikuchi, R. Maeda, T. R. Chung, and T. Suga, Appl. Phys. Lett. **68**, 2222 (1996) .
[16] C. Wang, E. Higurashi, and T. Suga, Jpn. J. Appl. Phys. **47**, 2526 (2008) .
[17] N. Shigekawa, N. Watanabe, and E. Higurashi, Proc. 3rd Int. IEEE Workshop Low-Temperature Bonding for 3D Integration, Tokyo, Japan, (IEEE, 2012), pp. 109-112.
[18] J. Liang, T. Miyazaki, M. Morimoto, S. Nishida, N. Watanabe, and N. Shigekawa, Appl. Phys. Express **6**, 021801 (2013) .
[19] J. Liang, S. Nishida, M. Morimoto and N. Shigekawa, Electron. Lett. **49**, 830 (2013).
[20] C. Lian, H. G. Xing, Y.-C. Chang, and N. Fichtenbaum, Appl. Phys. Lett. **93**, 112103 (2008).

© 2014 WILEY-VCH Verlag GmbH & Co. KGaA, Weinheim